ISSN 0915-633X

NATIONAL INSTITUTE FOR FUSION SCIENCE

Turbulent Transport and Structural Transition in Confined Plasmas

K. Itoh, S.- I. Itoh, A. Fukuyama and M. Yagi

(Received - Sep. 24, 1996)

NIFS-457 Oct. 1996

RESEARCH REPORT
NIFS Series

NAGOYA, JAPAN

Turbulent Transport and Structural Transition in Confined Plasmas

Kimitaka Itoh*, Sanae-I. Itoh†, Atsushi Fukuyama†† and Masatoshi Yagi†

** National Institute for Fusion Science, Nagoya 464-01, Japan*

† Research Institute for Applied Mechanics, Kyushu University, Kasuga 816, Japan

†† Faculty of Engineering, Okayama University, Okayama 700, Japan

Abstract

Theory of the far-nonequilibrium transport of plasmas is described. Analytic as well as simulation studies are developed. The subcritical nature of turbulence and the mechanism for self-sustaining are discussed. The transport coefficient is obtained. The pressure gradient is introduced as an order parameter, and the bifurcation from the collisional transport to the turbulent one is shown. The generation of the electric field and its influence on the turbulent transport are analyzed. The bifurcation of the radial electric field structure is addressed. The hysteresis appears in the flux-gradient relation. This bifurcation causes the multifold states in the plasma structure, driving the transition in transport coefficient or the self-generating oscillations in the flux. Structural formation and dynamics of plasma profiles are explained.

This is an invited paper for *International Conference on Plasma Physics* (Nagoya, 1996)

Key words: far-nonequilibrium system, turbulence, anomalous transport, gradient-flux relation, subcritical excitation, bifurcation, radial electric field, structural transition, entropy production rate, hysteresis

1. Introduction

Recently, progress has been made in the transport and structural formation in plasmas. Experimental observations have shown characteristic features of plasmas as the far-nonequilibrium system. Namely; (1) The relation between the "gradient" and "flux" is not linear; as is shown in Fig.1. The heat flux across the magnetic surface nonlinearly grows as the temperature gradient increases. (2) The interference between various fluxes and gradient takes place; the off-diagonal elements exist in transport matrix. (The Curie's law in transport is violated.) (3) The bifurcation of the structure appears; the two distinctive gradients are realized for similar heat flux like L- and H-modes [1]. (4) The burst of plasma flow is generated (e.g., ELMs, geosubstorm etc.) [2].

These transport phenomena have been thought to be caused by plasma instabilities. The traditional method is the mixing-length argument based on the linear instabilities [3]. This method is useful in the case of *supercritical* turbulence. Although some nonlinear simulations on ion dynamics, treating the ion-temperature-gradient mode [4], give understanding of the ion energy transport [5], tests have found difficulties in explaining the experimental observations [6]. It has been widely known, however, that there is *subcritical* turbulence in plasmas [7]. The plasma turbulence is self-sustained by the nonlinearity, for which the theoretical method has been developed [8].

In this paper, essential characteristics of the confined plasma as the nonlinear nonequilibrium media are discussed. The turbulent transport and structural transition are analyzed by analytic and simulational study. The *gradient* is found to work as the *order parameter*. The gradient-flux relation is not only nonlinear but also multifold. The entropy production rate is maximum for fixed profile. The transition in transport is caused by the combined dynamics of the electromagnetic field and plasma. Hysteresis exists in the electric field bifurcation, causing the transition as well as limit cycle oscillations. Global structural formations are explained. Through these analyses, the impact of the plasma physics to the modern science is illuminated.

2. Self-sustained Turbulence

2.1 Model and Renormalization

We start from the study of the transport caused by microscopic fluctuations. A small region of the confined plasma is modelled by a slab, and local coordinates (x, y, z) are used. (The x-axis is in the direction of gradient, and the z-axis is in the direction of main magnetic field.) In plasmas of our interest, the ratio of the plasma pressure to the magnetic pressure, β, is low, and the reduced set of equations [9] is used to describe the dynamics. The equation of motion, Ohm's law and the energy conservation equation are given as

$$\frac{\partial \nabla_\perp^2 \phi}{\partial t} + [\phi, \nabla_\perp^2 \phi] = \nabla_{||} J + (\Omega' \times \vec{\xi}) \cdot \nabla p + \mu_c \nabla_\perp^4 \phi \ , \tag{1}$$

$$\frac{\partial \Psi}{\partial t} = - \nabla_{||} \phi - \frac{1}{\xi} \left(\frac{\partial J}{\partial t} + [\phi, J] \right) + \lambda_c \nabla_\perp^2 J \ , \tag{2}$$

$$\frac{\partial p}{\partial t} + [\phi, p] = \chi_c \nabla_\perp^2 p \ . \tag{3}$$

where $[f, g] = (\nabla f \times \nabla g) \cdot \vec{b}$, ($\vec{b} = \vec{B}_0 / B_0$, B_0: main magnetic field), Ω': average curvature of the magnetic field, Ψ: vector potential, $\xi = (\delta/a)^{-2}$, δ: collisionless skin depth [10]. The resistivity is neglected. The transport coefficients μ_c, λ_c, χ_c are for the collisional diffusion, being the viscosity for the ion momentum, the current diffusivity and the thermal diffusivity, respectively. Length and time are normalized to the plasma radius a and poloidal Alfven transit time $\tau_{Ap} = qR/v_A$. Pressure and potential are normalized to $B_0^2 q^2 / 2\varepsilon\mu_0$ and $a v_{Ap} B_0$, ($\varepsilon = a/R$). The parallel mode number is given as $k_{||} = k_y s x$ where s is the shear parameter $s = q^{-1} r(dq/dr)$ and q is the safety factor.

The Lagrangian nonlinearity is renormalized. (Detailed procedure is given in [10].) We take a test mode (denoted by k). Taking direct interactions, the nonlinear term for the test mode, $[\phi, \bar{Y}]$, is written as $[\phi, \bar{Y}] \cong \Sigma [\phi_{-1}, [\phi_1, \bar{Y}]]$. (The suffix 1 indicates background fluctuations k_1.) Approximation $[\phi_{-1}, [\phi_1, \bar{Y}]] = \left(|\partial \phi_1 / \partial r|^2 \partial^2 \bar{Y} / r^2 \partial \theta^2 + |\partial \phi_1 / r \partial \theta|^2 \partial^2 \bar{Y} / \partial r^2 \right)$ is used. Equations $\partial \nabla_\perp^2 \phi / \partial t = \nabla_{||} J + (\Omega' \times \vec{\xi}) \cdot \nabla p + (\mu_N + \mu_c) \nabla_\perp^4 \phi$,

$\partial\Psi/\partial t = -\nabla_{\parallel}\phi - \xi^{-1}\partial J/\partial t + (\lambda_N + \lambda_c)\nabla_{\perp}^2 J$ and $\partial p/\partial t = (\chi_N + \chi_c)\nabla_{\perp}^2 p - [\phi, p_0]$ is reduced from Eqs.(1)-(3). (See [10] for expressions of $\{\mu_N, \lambda_N, \chi_N\}$.) Parameter G_0 is defined as $G_0 = \Omega' dp_0/dr$, and p_0 is the global pressure profile.

2.2 Dressed Test Mode

In the set of renormalized equations, each fluctuation mode is analyzed separately; the nonlinear interactions with background fluctuations are given by the turbulent coefficients $\{\mu_N, \lambda_N, \chi_N\}$. We call this analysis as "dressed test mode". The eigenvalue equation for marginal stability is given as

$$k_\theta^2 s^2 \frac{d}{dk}\frac{1}{(\lambda_c + \lambda_N)k_\perp^2}\frac{d}{dk}\phi(k) + (\mu_c + \mu_N)k_\perp^4\phi(k) - \frac{k_\theta^2 G_0}{(\chi_c + \chi_N)k_\perp^2}\phi(k) = 0 \qquad (4)$$

$(k_\perp^2 = k_y^2 + k^2)$ The coefficients $\{\mu_N, \lambda_N, \chi_N\}$, which are determined, in principle depend on the choice of the mode number. By noting this k-dependence, the spectrum of the turbulence could be obtained [11]. We here present the approximate solution based on the mean field approach, in which $\{\mu_N, \lambda_N, \chi_N\}$ are approximated as a single set of coefficients.

2.3 Steady State Turbulence: L-mode and H-mode

In the stationary state, relations $\mu_N(\mu_N + \mu_c) = \hat{\phi}^2$, $\mu_{eN}(\mu_{eN} + \mu_{ec}) = P^2\hat{\phi}^2$, $\lambda = (\delta/a)^2\mu_e$, $\chi_N(\chi_N + \chi_c) = Q^2\hat{\phi}^2$ and $\hat{\phi}^2 \equiv \Sigma|\phi_l|^2(2 + 2C)^{-1}$ hold. Coefficients P and Q are related to Prandtl numbers, vary much more slowly than the turbulence level, and are close to unity [12]. (Coefficient $C = (\xi k_{\parallel l}^2/(\mu_{eN} + \mu_{ec}) + G_0 k_{\theta l}^2/(\chi_N + \chi_c))k_{\perp l}^{-6}(\mu_N + \mu_c)^{-1}$ is of order unity.) The marginal stability condition was derived from Eq.(4) as

$$\Im \equiv G_0 s^{-4/3}(\lambda_N + \lambda_c)^{2/3}(\chi_N + \chi_c)^{-1}(\mu_N + \mu_c)^{-1/3} = \Im_c(k_y) \qquad (5)$$

The eigenvalue $\Im_c(k_y)$ takes the minimum value $\Im_{c,m}$ for the least stable mode, where $\Im_{c,m}$ is the critical Itoh number which is of the order of unity. In the strong turbulence limit,

$\mu_N >> \mu_c$, $\mu_N >> \mu_c$ and $\chi_N >> \chi_c$, Eq.(5) gives $\chi_N = \Im_{c,m}^{-3/2} G_0^{3/2} s^{-2} (\delta/a)^2 P/\sqrt{Q}$. The coefficient $P/\sqrt{Q}\Im_{c,m}^{3/2}$ is close to unity, and the thermal transport coefficient in the L-mode plasma χ_L has been estimated as

$$\chi_L \simeq G_0^{3/2} s^{-2} (\delta/a)^2 \tag{6}$$

This result is confirmed by the scale invariance method [13]. The transport coefficient is an increasing function of the gradient. The typical mode number scales as $k_\perp \sim G_0^{-1/2} sa\omega_p/c$. The turbulent energy follows the relation $\langle W_{\nabla\phi, j, p} \rangle \propto G_0^2$. The gradient parameter G_0 characterizes this nonlinear nonequilibrium system. Contrary to the systems near the thermal equilibrium, in which fluctuations are the thermal fluctuations [14], the enhanced fluctuations are controlled by the parameter G_0. The *nonlinear* nature of the flux against the gradient is derived.

In the presence of the inhomogeneous radial electric field, the similar argument has been developed [15]. The result was obtained as

$$\chi_H \equiv \left(1 + 0.52 G_0^{-1} \omega_{E1}^2\right)^{-1} \chi_L \tag{7}$$

where $\omega_{E1} = E_r' \tau_{Ap}/B$. The fluctuation is reduced in the presence of the inhomogeneous radial electric field [16] (see also review [17]).

2.4 Subcritical Excitation

Equation (5) determines the fluctuation level and turbulent transport coefficient as a function of the equilibrium pressure gradient, i.e., $\tilde{\phi}(G_0)$ and $\chi(G_0)$. The linear instability condition is obtained as $G_0 \geq G_c$ with $G_c = \Im_{c,m} (sa\omega_p/c)^{4/3} \chi_c \mu_c^{1/3} \chi_{ec}^{-2/3}$, from Eq.(5) by taking $\mu_N = \lambda_N = \chi_N = 0$. By expanding Eq.(5) near $G_0 \simeq G_c$, we have $\tilde{\phi}^2 = -(3\mu_{ec}^2/2P^2)(G_0/G_c - 1)$, using the relations $\mu_c \simeq \chi_c$ and $\mu_{e,c}/\chi_c \sim \sqrt{m_e/m_i}$ for collisional diffusion (m_e/m_i : mass ratio). This is the backward bifurcation. Finite amplitude of ϕ is

expected below the critical pressure gradient, $G_0 < G_c$. The branch of the large fluctuation amplitude is obtained as Eq. (6). These two branches merge at a critical pressure gradient, $G_0 = G_*$,

$$G_0 = G_* \cong \Im_{c,m}(2sa\omega_p/c)^{4/3}\chi_c^{2/3} . \tag{8}$$

Figure 2 illustrates the theoretical prediction of the fluctuation level as a function of the pressure gradient, G0. Multifold forms of $\tilde{\phi}(G_0)$ and $\chi(G_0)$ are seen.

Anomalous transport is predicted to occur if G_0 exceeds the critical value $G*$, which is smaller than the linear stability boundary G_c. Normalized number $\Im = (q/s)^{4/3}G_0\lambda^{2/3}\chi^{-1}\mu^{-1}$ is compared to Rayleigh number in the Bernard cell problem $\Re_a = Ag_r d^4 \nabla T \nu_c^{-1}\chi_c^{-1}$ (d: distance of two plates, Agr: buoyancy by gravity). What is noticeable for plasmas is that the dissipation, through the current diffusivity (i.e., the electron viscosity), can *enhance* the driving force.

2.5 Maximum Entropy Production Rate

The entropy production rate $\wp$ is known to be minimum in the non-equilibrium state close to the thermal equilibrium [18]. This is also the case for the collisional transport in plasmas [19]. However, the quantity $\wp$ takes the maximum in the self-sustained turbulence.

From Eqs.(1)-(3), we have an integral form as [20]

$$\int dV\sigma \equiv \mu_c\int dV|\nabla_\perp^2\phi|^2 + \lambda_c\int dV|\nabla_\perp J|^2 + \chi_c\int dV|\nabla_\perp p|^2 = -(\Omega' + dp_0/dr)\int dV q_r$$

(σ: dissipation, q_r: heat flux.) in the steady state. The entropy production rate per unit volume, $\wp = \sigma T^{-2}$, is expressed as $\wp = -T^{-2}(\Omega' + dp_0/dr)q_r$. From Eq.(5), the heat flux $q_r = -\chi_N \nabla p_0$ is given in terms of the fluctuations as $q_r = -G_0^{3/2}s^{-2}(\delta/a)^2\nabla p_0\Im_c(k_y)^{-3/2}$. The entropy production rate is given as a functional of fluctuations, for fixed gradient, as

$$\wp = \left\{T^{-2}\left(\Omega' + dp_0/dr\right)\chi_L dp_0/dr\right\}\left(\Im_{c,m} / \Im_c(k_y)\right)^{3/2} \qquad (9)$$

The analysis has shown that the stationary turbulent state is determined by the least stable mode and $\Im_c(k_y)$ is minimized; $\wp$ is *maximized* as the turbulence grows to the stationary state. The production rate in turbulent transport is greater than that in the collisional transport by factor of $\left(1 + \Omega'(dp_0/dr)^{-1}\right)\chi_L\chi_c^{-1}$. The maximum entropy production rate is also the characteristics that discriminate the nonlinear non-equilibrium transport from the linear one. The division of the dissipated energy between electrons and ions was found to be nearly equal [21].

2.6 Nonlinear Simulation

Direct nonlinear simulation of the basic set of equations (1)-(3) was performed [20]. The two-dimensional turbulence has been calculated in a system of the size $|x| < L_x$ and $|y| < L_y$. Parameters in the normalized form are: $\mu_c = \chi_c = 0.2(c/a\omega_p)^2$, $\mu_{e\,c} = 0.01(c/a\omega_p)^2$, $s = 0.5$, $L_x = 40(c/a\omega_p)$ and $L_y = 6.4\pi(c/a\omega_p)$. For this set of parameters, the linear stability boundary is given as $G_c \simeq 0.4$, i.e., $\Im_{c,m} \simeq 0.4$. The periodicity condition is taken in the y-direction, and M=64 modes are taken in ky-space ($k_{y,min} = 10/64$ and $k_{y,max} = 10$). The $\partial\Psi/\partial t$ term in the Ohm's law Eq.(2) is neglected to illuminate the nonlinear mechanism of the instability. The back-ground modification, i.e., the change of the ky=0 component, is omitted.

Nonlinear excitation was confirmed in the simulation. Figure 3(a) shows the time evolution of the fluctuation amplitude as a function of time for the case of $G_0 = 0.5$. In the small amplitude limit, the perturbation grows following the linear growth rate $\gamma_L \sim 0.17$. However, when the amplitude exceeds a threshold value, $< W_\phi > \sim 10^{-4}(c/a\omega_p)^2$, the growth rate starts to increase. ($< W_\phi > = L_x^{-1}\Sigma\int dx|\nabla_\perp\phi(x,k_y)|^2 B_0^{-2}$ is the square of the average fluctuation velocity.) In the time range of $35 < t < 50$, the growth rate becomes larger as the amplitude increases. This is the nonlinear destabilization through the electron dynamics. When amplitude becomes much larger, the growth rate starts to decrease, showing the saturation.

(The dashed line shows the case in which the $[\phi,j]$ term in Eq.(2) is omitted.) The threshold of nonlinear excitation, $< W_\phi > \sim 10^{-4}(c/a\omega_p)^2$ is in the range of the theoretical prediction

The fluctuation level is illustrated as a function of the gradient parameter in Fig.3(b). We see that the steady state turbulence is realized even below the critical pressure gradient against the linear instability, $G_c \simeq 0.4$. The critical amplitude for the nonlinear excitation is much smaller than the saturation level itself. The simulation demonstrates clearly the subcritical nature of the plasma turbulence. It is also emphasized that the fluctuation level is insensitive to the linear growth rate.

3. Bifurcation and Transition

3.1 L-H Transition

The spontaneous establishment of steep gradient at edge was found in the ASDEX experiment, and is called as *H-mode* [1]. The mechanism of the transition has been proposed in the form of the radial electric field bifurcation [22]. The problem of the electric field and transport is a typical example for the global self-sustaining structure.

The generation and bifurcation of the radial electric field have been investigated [17]. If one writes the equation, for singly charged ions, one has

$$\varepsilon_0\varepsilon_\perp e^{-1}\frac{\partial}{\partial t}E_r = \Gamma_{e-i}^{anom} - \Gamma_i^{lc} - \Gamma_i^{bv} - \Gamma_i^{v\nabla v} - \Gamma_i^{NC} + \Gamma_e^{NC} - \Gamma_i^{cx} \qquad (10)$$

The terms on the right hand side are (see, e.g. [17, 22-25]); (i) Γ_{e-i}^{anom} (bipolar part of the anomalous cross field flux), (ii) Γ_i^{lc} (loss cone loss of ions), (iii) Γ_i^{bv} (bulk viscosity coupled to the magnetic field inhomogeneity), (iv) $\Gamma_i^{v\nabla v}$ (Reynolds stress in the global flow), (v) Γ_i^{NC}, Γ_e^{NC} (collisional fluxes) and (vi) Γ_i^{cx} (ion loss by the charge exchange), respectively.

Bifurcations of the hard transition type have been found from Eq.(10) [22,23]. As the parameter λ_p $(\rho_p(n'/n + \alpha_E T'/T))$ increases, the electric field shows the bifurcation from the branch with weak electric field to the one with strong field. The neutral density or the viscosity plays the role of controlling parameter that modifies the bifurcation.

Cusp-type catastrophe is constructed as Figure 4. The rapid change of E_r was confirmed at the transition [26], and the nonlinear dependence of the radial current on E_r was observed [27]. Numerical simulation has shown that as the fluctuations develop, a zonal flow is generated (See references in [17]).

3.2 Interface and Meso-phase

The spatial structure has vital importance, because the inhomogeneity of the radial electric field reduces the transport as in Eq.(7). The interface at the spatial discontinuity in media which has multiple states (the L- and H-phases in this case) is studied. As plasma parameters gradually change with radius, there could appear an interface, across which the different branches of the solution touch. The two branches are connected by a layer of finite width due to the viscosity. This layer is called a *meso-phase*. The layer was found to be thermodynamically stable in the case of neoclassical theory [28]. For the parameter g, that represents the variable in the abscissa of Fig.4, we have $\Delta\Phi(g) \equiv \int_{X_l}^{X_u} \{\Gamma_e[X;g] - \Gamma_i[X;g]\}\, dX = 0$ at the interface (X_u and X_l are the solution X[g] on the upper branch and lower branch, respectively). This relation is the counterpart of the *Maxwell's construction* (Maxwell's Rule of Equal Areas) at the phase transition in the thermodynamics [29]. The thickness of the interface layer is evaluated as $\delta \sim \sqrt{\hat{\rho}_p^2 + \mu_\perp/\nu_*}$, where $\hat{\rho}_p$ is the squeezed poloidal gyro-radius, and the viscosity $\mu_\perp$ is given by Eq.(7). The transport coefficient $\mu_\perp$ depends on the sharpness of the gradient. If the viscosity is reduced, the interface becomes thinner, and as a consequence, the viscosity is further reduced. This system thus 'self-organizes' the thin transport barrier via the interactions of the electric field and the transport coefficient.

3.3 Dithering ELMs

The system of dynamical equations for the plasma parameters, radial electric field and transport coefficient is formulated as the time-dependent Ginzburg-Landau (TDGL) type. A limit cycle oscillation, i.e., the sequence of the transitions and back transitions, is predicted [30]. The parameter g, which controls the transport, was chosen as $g \equiv \rho_p \tilde{D}_L L_n^{-1} \nu_i^{-1} \rho_p^{-2}$ and

the current (right hand side of Eq.(10)) is modelled by a quadratic equation of E_r. Figure 5 illustrates the limit cycle oscillation seen in the flux out of the plasma. The H-phase and L-phase are realized one by one; in each of the stages, the radial profile of the transport coefficient is one of those. This is the self-organized oscillation generated by the hysteresis and hard transition in the plasma transport and electric field generation. Under a constant supply of plasma from core, the oscillation is possible near the threshold condition of the L-H transition. Small and frequent ELMs are observed experimentally near the threshold power for the L-H transition [2], and are called as dithering ELMs. These oscillations can also be found in the zero-dimensional models (e.g., [30,24]). The appearance of this oscillation is studied under the slow time evolution of the global plasma parameter [31].

As the plasma parameters reach the threshold conditions, the oscillation amplitude jumps abruptly from zero to finite value and from finite amplitude to zero. The bifurcation to ELMs is stronger than those in Hopf-bifurcation. This feature is characteristic of the hard type of bifurcation which contains a hysteresis.

4. Structural Formation

4.1 L-mode Plasma

In the nonlinear-nonequilibrium systems, like the confined plasmas, the turbulent transport coefficient is dependent on the structure itself. As a result of the structure-dependence of the transport, there appear various structures. The self-sustained structure is analyzed by the turbulent transport theory.

The method of Chapter 2 has been applied to tokamaks, for which many data on the plasma profiles are available. The formula was given as [32]

$$\chi_{TB} = C_{TB}\, q^2 f(s,\alpha)^{-1} (-R\beta')^{3/2} (c/\omega_p)^2 v_A R^{-1} \qquad (11)$$

where $f(s,\alpha) = (1+\kappa)^{-5/2}\sqrt{2(1-2s')[1-2s'+3s'^2(1+\kappa)]}$, κ is the average good curvature and $s' = s - \alpha$, $\alpha = -Rq^2\beta'$. By choosing the numerical constant C_{TB} as $C_{TB} \simeq 10$, the L-mode and the improved confinement were simulated.

Transport simulation, in which the temperature and current profiles are solved for given density profile, was performed for the OH heating and additional heating. In both cases, the thermal conductivity increases near the plasma edge. The shapes of the electron temperature profile are similar in OH and additional heating cases, to recovering the *profile resilience*. Dependence of the energy confinement time on various parameters reproduces experimental observations [33].

5.2 Internal Transport Barrier

In addition to the electric field bifurcation, there is another mechanism to generate the transport barrier. The form Eq.(11) shows that strongly-reduced magnetic shear can make the transport coefficient smaller [34]. The effect of the reduced shear on the linear stability was pointed out in [35], followed by recent theoretical work. Equation (11) shows that the nonlinear instability and turbulence are suppressed by the reduced magnetic shear, $s < 0.3$.

An example of this result is shown in Fig.6. The transport barrier could be established either at the edge or in the core. The model was also applied to the High-β_p mode or PEP-mode. When the plasma beta exceeds the threshold value, i.e., $\beta_p > 1$, the internal transport barrier is shown to appear. The Shafranov shift and the Bootstrap current are large if the pressure gradient becomes steeper, and reduce the anomalous transport coefficient to generate the internal transport barrier. The increment in sheared rotation can then further reduce the transport coefficients, which in turn strengthens the improvement. Through this link of the mutual interactions, the internal transport barrier was predicted to be established, besides the edge transport barrier. This structural formation has strong impact on the perspective of the igniting plasmas [36].

4.3 Peaked Profile Mode

The structure formation of the plasma can also be observed in the density profile. The peaking of the plasma density is modelled in combination with the radial electric field [37]. Density peaking without a central particle source is an example of the interface of various kinds of fluxes. The possibility is pointed out that the peaked profile of the radial electric field, which is generated by the peaked density, enhances the inward pinch through the anomalous viscosity. A reduced neutral density is essential for it, because the neutrals tend to reduce the radial electric field. This is compared with the nature of the Improved Ohmic Confinement (IOC) which is realized by shutting-off the gas puff. The evolution associated with co-and counter NBI heating was simulated [38].

5. Further Problems

Although progress has been made, there remain couple of fundamental problems.

The transport coefficients like (11) is given in terms of the local parameter. The variation propagates in the radial direction with the time scale of the confinement time. In addition to this kind of slow propagation of change, there is the possibility of a fast propagation of change takes place (e.g., after the L-H transition, the pellet injection, sawtooth, X-events, etc.). The radial transmission of turbulence itself was studied by the method of TSDIA [39]. In order to study this kind of fast propagation, models have been proposed, based on an avalanche of bifurcation or on dynamics near marginal stability or dynamics of global modes [40]. This area clearly demands future intensive study.

The magnetic perturbation is important if the magnetic braiding takes place. In the braided magnetic surfaces, electrons are subject to the faster loss [41]. This selective loss of electron momentum then induces the stronger self-sustained turbulence [42]. (Note that Eq.(6) is in proportion to $\lambda/\sqrt{\mu\chi}$). The nonlinear simulation has also supported the stronger turbulence in the presence of the magnetic braiding [43]. The magnetic stochasticity onsets if the level of turbulence exceeds the threshold level. This nature of discontinuity explains the abrupt occurrence of events at the beta-limit. One of the example is the Giant ELMs (type-I ELM [2]). It is shown that, if the pressure gradient reaches the critical value,

$\alpha = \alpha_c \sim s/2$, the bifurcation in turbulent transport takes place. This is the turbulence-turbulence transition, and is associated with the hysteresis [44]. This hysteresis can lead to the limit cycle oscillation, accompanied by the bursts of the turbulence and plasma fluxes. When a transition takes place at a certain radius, the resultant large heat flux induces the transition at the neighbouring surfaces. The avalanche of transitions occurs. The propagation of avalanche is analyzed [45].

6 Summary

Essential feature of the nonlinear nonequilibrium transport in confined plasmas is illustrated. The "*gradient*" is taken into as the *order parameter*, and the fluctuation level, correlation length and transport coefficients are expressed in terms of the gradient. The self-sustained turbulence occurs as a subcritical turbulence. The transition from the linear-nonequilibrium transport is shown, and the maximum entropy production rate is illustrated. Difference is stressed from the diffusion which is generated by the thermal fluctuations. The electric field bifurcation is explained. The gradient-flux relation not only has nonlinearity but also is multifold. Mechanisms causing the plasma structure, e.g., transport barriers, are discussed. The hysteresis provides the self-generated oscillation of the structure, being accompanied by the bursts of plasma flow. These result provide a prototypical view for the far nonequilibrium systems.

The understanding of the turbulent transport and structural transition in plasmas was advanced, but much theoretical efforts are required to fully understand the nature of plasmas.

Acknowledgements

Authors acknowledge Dr. M. Azumi, Dr. J. W. Connor, Prof. A. J. Lichtenberg, Prof. T. Ohkawa, Dr. H. Sanuki, Dr. K. C. Shaing, Prof. F. Wagner for various discussions. This work is partly supported by the Grant-in-Aid for Scientific Research of Ministry of Education, Science, Culture and Sports, Japan, by the collaboration programme of National

Institute for Fusion Science and by the collaboration programme of Advanced Fusion Research Center of Kyushu University. They also thank Max-Planck-Institut fur Plasmaphysik for hospitality during their visit.

References

[1] Wagner F *et al* . 1982 *Phys. Rev. Lett.* **49** 1408.

[2] ASDEX Team 1989 *Nucl Fusion* **29** 1959.

[3] Kadomtsev B B 1965 *Plasma Turbulence* (Academic Press, New York).

[4] Coppi B, Rosenbluth M N and Sagdeev R Z 1967 Phys. Fluids **10** 582; Kadomtsev B B and Pogutse O P 1970 *Reviews of Plasma Physics* (Consultants Bureau, New York) Vol.5 p249.

[5] See e.g., Waltz R E, Kerbel G D, Milovich J 1994 *Phys. Plasmas* **1** 2229, and Dimits A M, Williams T J, Byers J A and Cohen B I 1996 Phys. Rev. Lett. **77** 71.

[6] Connor J W et al. 1994 *Plasma Phys. Contr. Fusion* **36** 319.

[7] See, e.g., Hirshman S P and Molvig K 1979 *Phys. Rev. Lett.* **42** 648.

[8] Itoh K, Itoh, S-I and Fukuyama A 1992 *Phys. Rev. Lett.* **69** 1050.

[9] Strauss H R 1977 *Phys. Fluids* **20** 1354.

[10] Itoh K, et al. 1994 *Plasma Phys. Contr. Fusion* **36** 279 and 1501.

[11] Itoh S-I and Itoh 1996 "*Theory of fully-developed turbulence in buoyancy-driven fluids and ion pressure-gradient driven plasmas*" submitted to *Phys. Rev. E.*

[12] Itoh K, Itoh S-I, Fukuyama A, Yagi M and Azumi M 1993 *J. Phys. Soc. Jpn.* **62** 4269.

[13] Connor J W 1993 *Plasma Phys. Contr. Fusion* **35** 757.

[14] Kubo R 1957 *J. Phys. Soc. Jpn.* **12** 570.

[15] Itoh S-I et al. 1994 *Phys. Rev. Lett.* **72** 1200; *Plasma Phys. Contr. Fusion* **36** 123.

[16] Itoh S-I et al. 1989 in *Plasma Physics and Controlled Nuclear Fusion Research 1988* (IAEA, Vienna) Vol.2 p23; Shaing K C *et al* 1989 *ibid.*, p13; Biglari H et al. 1990 *Phys. Fluids B* **2** 1.

[17] Itoh K and Itoh S-I 1996 *Plasma Phys. Contr. Fusion* **38** 1.

[18] Prigogine I 1961 "*Introduction to Thermodynamics of Irreversible Processes*" (2nd ed., Wiley-Interscience, New York) Chap. VII.

[19] Rosenbluth M N, Hazeltine R D, Hinton F L 1972 *Phys. Fluids* **15** 116.

[20] Yagi M et al. 1995 *Phys. Plasmas* **2** 4140.

[21] Itoh S-I et al. 1994 *Phys. Plasmas* **1** 1154.

[22] Itoh S-I, Itoh K 1988 *Phys. Rev. Lett.* **60** 2276.

[23] Shaing K C, Crume E Jr. 1989 *Phys. Rev. Lett.* **63** 2369.

[24] Diamond P H, Liang Y-M, Carreras B A, Terry P W 1994 *Phys. Rev. Lett.* **72** 2565.

[25] Drake J F *et al* 1992 *Phys. Fluids B* **4** 488;
Rozhanskii V, Tendler M 1992 *Phys. Fluids B* **4** 1877;
Stringer T E 1993 *Nucl. Fusion* **33** 1249;
Yoshizawa A 1991 *Phys. Fluids B* **3** 2723.
Toda S et al. 1996 presented at *International Conference on Plasma Physics* (Nagoya) 9E09.

[26] Groebner R J, Burrell K H, Seraydarian 1990 *Phys. Rev. Lett.* **64** 3015.
Ida K et al. 1990 *Phys. Rev. Lett.* **65** 1364.

[27] Weynants R R *et al* 1992 *Nucl. Fusion* **32** 837.

[28] Hastings D E, Hazeltine R D, Morrison P J 1986 *Phys. Fluids* **29** 69;
Yahagi E, Itoh K, Wakatani M 1988 *Plasma Phys. Contr. Fusion* **30** 1009;
Shaing K C 1984 *Phys. Fluids* **27** 1567.

[29] Haken H 1976 *Synergetics* (Springer Verlag, Berlin) Section 9.3.

[30] Itoh S-I et al. 1991 *Phys. Rev. Lett.* **67** 2485; 1993 *Nucl. Fusion* **33** 1445.

[31] Zohm H 1994 *Phys. Rev. Lett.* **72** 222.

[32] Fukuyama A et al. 1994 *Plasma Phys. Contr. Fusion* **36** 1385; and 1995 **37** 611.

[33] Takizuka T 1992 *19th Europe. Conf. Contr. Fus. Plasma Heating* (Innsbruck) vol.16C, pt.II, p51.

[34] Yagi M et al. 1994 *J. Phys. Soc. Jpn.* **63** 10.

[35] Kadomtsev B B and Pogutse O P 1970 *ibid.* 321.

[36] Fukuyama A et al. 1995 *Nucl. Fusion* **35** 1669.

Tateishi G et al. 1996 presented at *International Conference on Plasma Physics* (Nagoya) 9U03.

[37] Itoh S-I 1990 *J. Phys. Soc. Jpn.* **59** 3431.

[38] Fukuyama A, Fuji Y, Itoh K, Itoh S-I 1994 *Plasma Phys. Contr. Fusion* **36** A159.

[39] Yoshizawa A 1985 *Phys. Fluids* **28** 1377.

[40] Kadomtsev B B, Itoh K, Itoh S-I 1995 *Comments Plasma Phys. Contr. Fusion* **17** 335;

Diamond P H, Hahm T S 1995 *Phys. Plasmas* **2** 3640;

Garbet X and Waltz R E 1996 *Phys. Plasmas* **3** 1898.

[41] Rechester A B, Rosenbluth M N 1978 *Phys. Rev. Lett.* **40** 38.

[42] Itoh K, Fukuyama A, Itoh S-I, Yagi M 1995 *Plasma Phys. Contr. Fusion* **37** 707.

[43] Yagi M et al. 1996 presented at *First Asia-Pacific Plasma Theory Conference* (Taejeon, Korea).

[44] Itoh S-I, Itoh K, Fukuyama A, Yagi M 1996 *Phys. Rev. Lett.* **76** 920.

[45] Kubota T et al. 1996 presented at *International Conference on Plasma Physics* (Nagoya) 9B19.

Figure Captions

Fig.1 Heat flux as a function of the temperature gradient.

Fig.2 χ_N and $\tilde{\phi}$ (normalized to χ_c) vs G_0 (normalized to $(sa\omega_p/c)^{4/3}\chi_c^{2/3}$.)

Fig.3 Temporal evolution of the fluctuation amplitude $< W_\phi >$ as a function of time (a). Fluctuation level vs G_0 (b). Fluctuations grow in regions (1)-(3). Subcritical appearance of the turbulence is explicitly shown. (From [20])

Fig.4 Relation between gradient and flux. The cusp-type bifurcation with hard transition is summarized.

Fig.5 Periodic formation and destruction of the edge transport barrier. Spatio-temporal evolution of effective diffusivity is shown. Periodic bursts of the outflow takes place. Here, length and time are normalized to ρ_p and ρ_p^2/D_L, respectively. (Quoted from [30].)

Fig.6 Radial profile (pressure, current and χ) with internal transport barrier. (a = 1m, R = 3m, B = 3T, $n_e(0) = 5 \times 10^{19} m^{-3}$, I_p =1MA, and P = 20 MW). (Quoted from [34].)

Fig.1

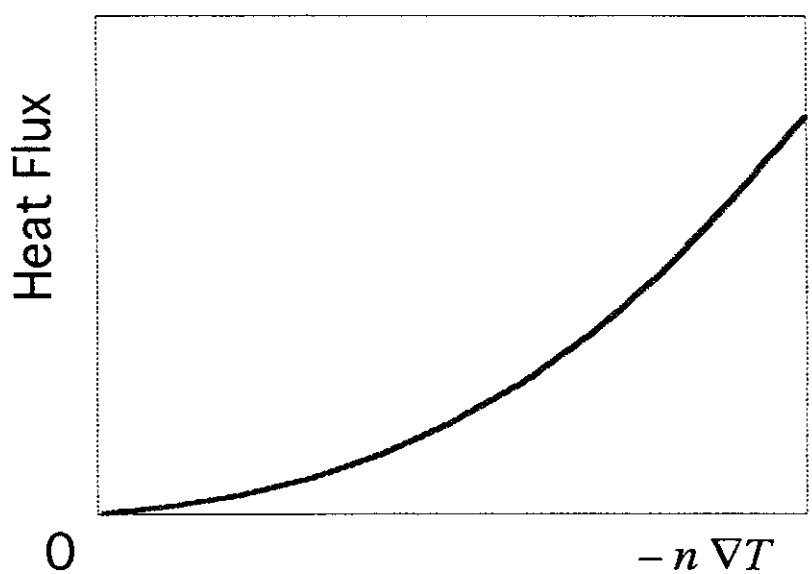

Fig.2

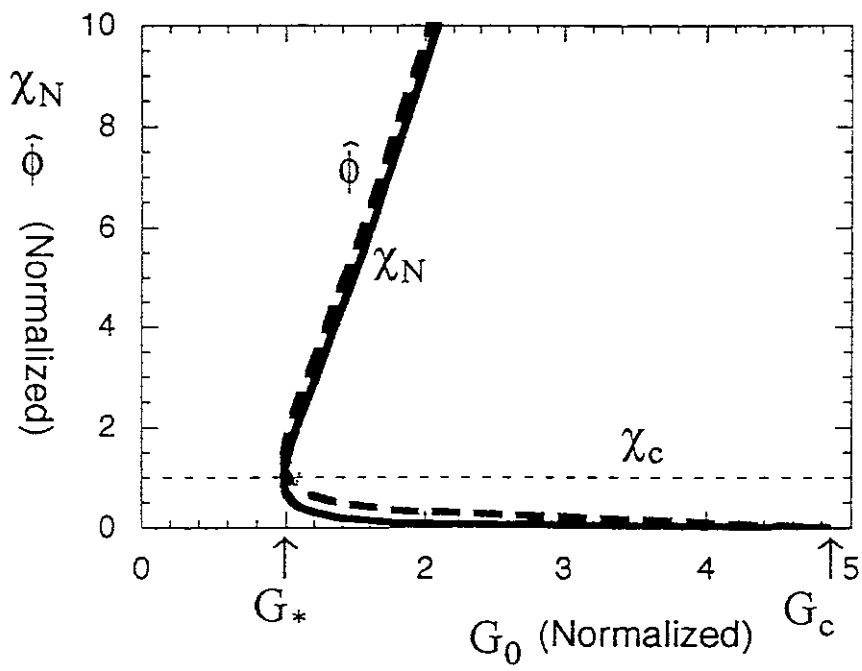
10
8
6
4
2
0
$\chi_N \hat{\phi}$ (Normalized)
$\hat{\phi}$
χ_N
χ_c
0
2
3
4
5
G_*
G_0 (Normalized)
G_c

Fig.3

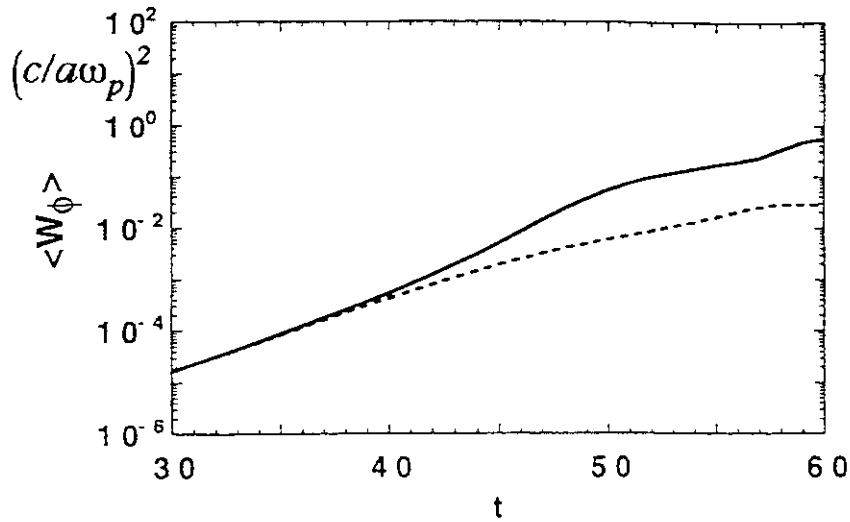
10^2
$(c/a\omega_p)^2$
10^0
10^{-2}
10^{-4}
10^{-6}
$\langle W_\phi \rangle$
30
40
50
60
t

(a)

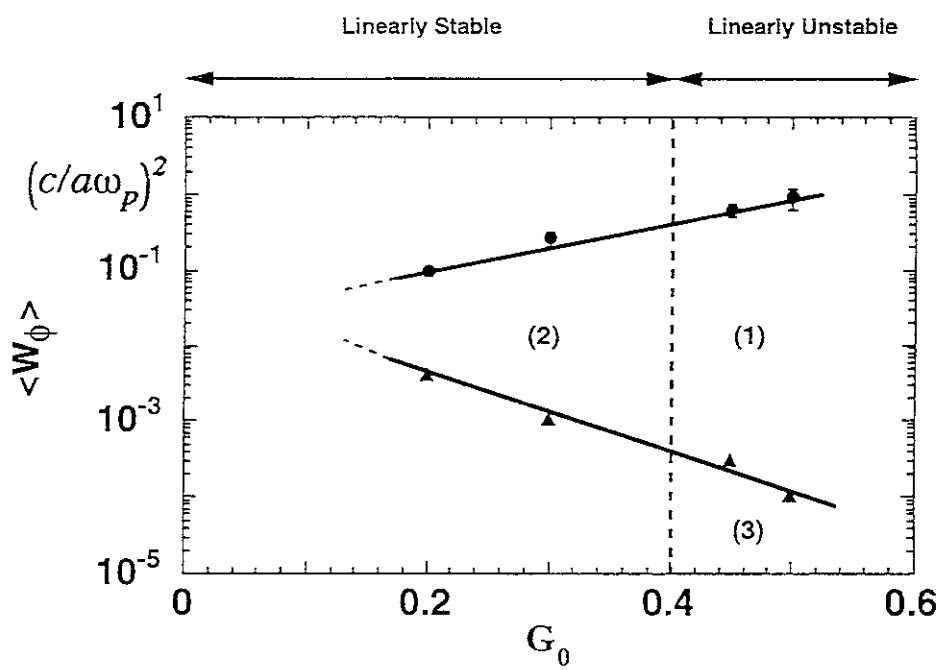
Linearly Stable
Linearly Unstable
10^1
$(c/a\omega_p)^2$
10^{-1}
10^{-3}
10^{-5}
$\langle W_\phi \rangle$
(2)
(1)
(3)
0
0.2
0.4
0.6
G_0

(b)

Fig.4

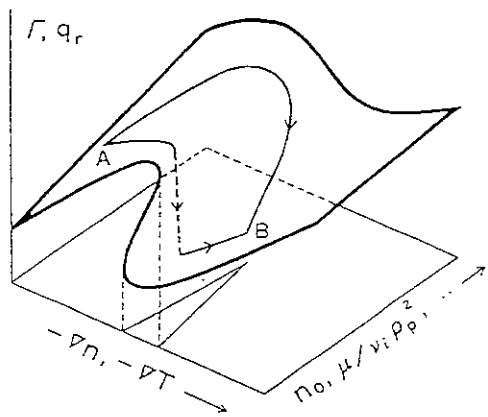

Fig.5

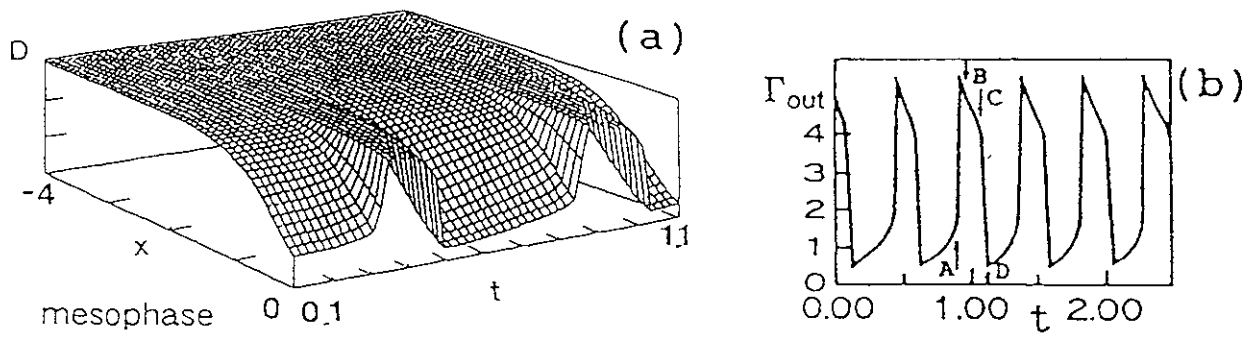

Fig.6

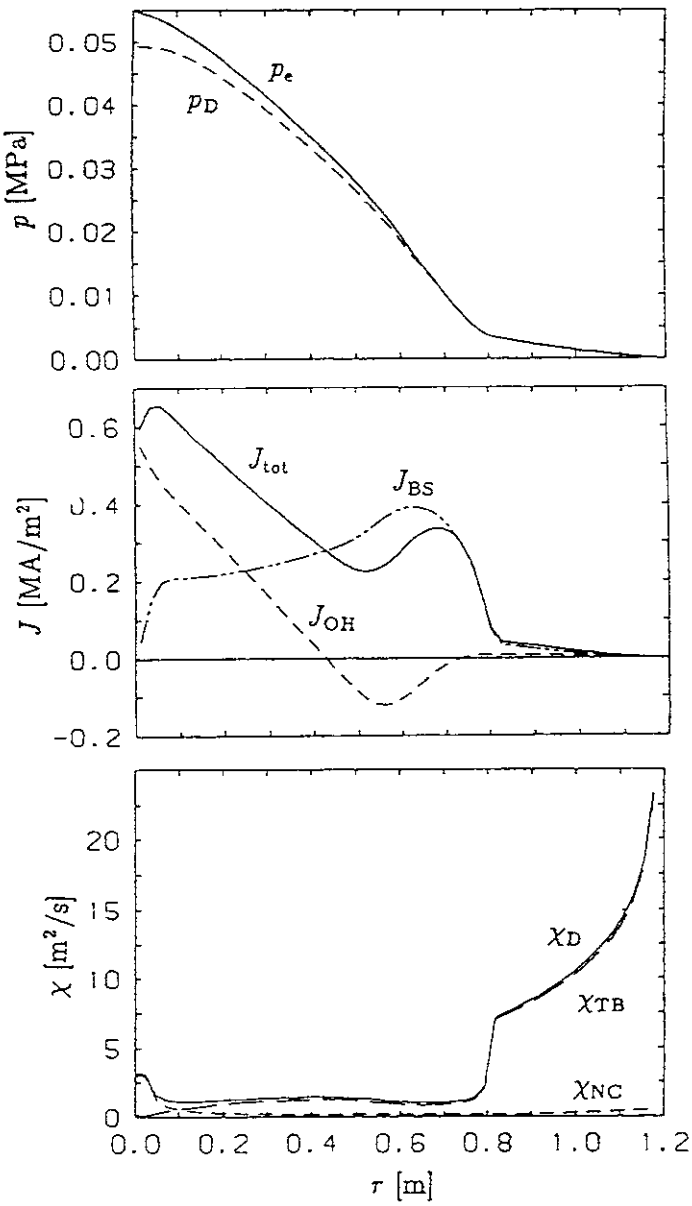
0.05
0.04
0.03
0.02
0.01
0.00
p [MPa]
p_e
p_D
0.6
0.4
0.2
0.0
-0.2
J [MA/m²]
J_{tot}
J_{BS}
J_{OH}
20
15
10
5
0
χ [m²/s]
χ_D
χ_{TB}
χ_{NC}
0.0
0.2
0.4
0.6
0.8
1.0
1.2
r [m]

Recent Issues of NIFS Series

NIFS-420 Y.N. Nejoh,
Arbitrary Amplitude Ion-acoustic Waves in a Relativistic Electron-beam Plasma System; July 1996

NIFS-421 K. Kondo, K. Ida, C. Christou, V.Yu.Sergeev, K.V.Khlopenkov, S.Sudo, F. Sano, H. Zushi, T. Mizuuchi, S. Besshou, H. Okada, K. Nagasaki, K. Sakamoto, Y. Kurimoto, H. Funaba, T. Hamada, T. Kinoshita, S. Kado, Y. Kanda, T. Okamoto, M. Wakatani and T. Obiki,
Behavior of Pellet Injected Li Ions into Heliotron E Plasmas; July 1996

NIFS-422 Y. Kondoh, M. Yamaguchi and K. Yokozuka,
Simulations of Toroidal Current Drive without External Magnetic Helicity Injection; July 1996

NIFS-423 Joong-San Koog,
Development of an Imaging VUV Monochromator in Normal Incidence Region; July 1996

NIFS-424 K. Orito,
A New Technique Based on the Transformation of Variables for Nonlinear Drift and Rossby Vortices; July 1996

NIFS-425 A. Fujisawa, H. Iguchi, S. Lee, T.P. Crowley, Y. Hamada, H. Sanuki, K. Itoh, S. Kubo, H. Idei, T. Minami, K. Tanaka, K. Ida, S. Nishimura, S. Hidekuma, M. Kojima, C. Takahashi, S. Okamura and K. Matsuoka,
Direct Observation of Potential Profiles with a 200keV Heavy Ion Beam Probe and Evaluation of Loss Cone Structure in Toroidal Helical Plasmas on the Compact Helical System; July 1996

NIFS-426 H. Kitauchi, K. Araki and S. Kida,
Flow Structure of Thermal Convection in a Rotating Spherical Shell; July 1996

NIFS-427 S. Kida and S. Goto,
Lagrangian Direct-interaction Approximation for Homogeneous Isotropic Turbulence; July 1996

NIFS-428 V.Yu. Sergeev, K.V. Khlopenkov, B.V. Kuteev, S. Sudo, K. Kondo, F. Sano, H. Zushi, H. Okada, S. Besshou, T. Mizuuchi, K. Nagasaki, Y. Kurimoto and T. Obiki,
Recent Experiments on Li Pellet Injection into Heliotron E; Aug. 1996

NIFS-429 N. Noda, V. Philipps and R. Neu,
A Review of Recent Experiments on W and High Z Materials as Plasma-Facing Components in Magnetic Fusion Devices; Aug. 1996

NIFS-430 R.L. Tobler, A. Nishimura and J. Yamamoto,
Design-Relevant Mechanical Properties of 316-Type Stainless Steels for Superconducting Magnets; Aug. 1996

NIFS-431 K. Tsuzuki, M. Natsir, N. Inoue, A. Sagara, N. Noda, O. Motojima, T. Mochizuki, T. Hino and T. Yamashina,
Hydrogen Absorption Behavior into Boron Films by Glow Discharges in Hydrogen and Helium; Aug. 1996

NIFS-432 T.-H. Watanabe, T. Sato and T. Hayashi,
Magnetohydrodynamic Simulation on Co- and Counter-helicity Merging of Spheromaks and Driven Magnetic Reconnection; Aug. 1996

NIFS-433 R. Horiuchi and T. Sato,
Particle Simulation Study of Collisionless Driven Reconnection in a Sheared Magnetic Field; Aug. 1996

NIFS-434 Y. Suzuki, K. Kusano and K. Nishikawa,
Three-Dimensional Simulation Study of the Magnetohydrodynamic Relaxation Process in the Solar Corona. II.; Aug. 1996

NIFS-435 H. Sugama and W. Horton,
Transport Processes and Entropy Production in Toroidally Rotating Plasmas with Electrostatic Turbulence; Aug. 1996

NIFS-436 T. Kato, E. Rachlew-Källne, P. Hörling and K.-D Zastrow,
Observations and Modelling of Line Intensity Ratios of OV Multiplet Lines for 2s3s 3S1 - 2s3p 3Pj; Aug. 1996

NIFS-437 T. Morisaki, A. Komori, R. Akiyama, H. Idei, H. Iguchi, N. Inoue, Y. Kawai, S. Kubo, S. Masuzaki, K. Matsuoka, T. Minami, S. Morita, N. Noda, N. Ohyabu, S. Okamura, M. Osakabe, H. Suzuki, K. Tanaka, C. Takahashi, H. Yamada, I. Yamada and O. Motojima,
Experimental Study of Edge Plasma Structure in Various Discharges on Compact Helical System; Aug. 1996

NIFS-438 A. Komori, N. Ohyabu, S. Masuzaki, T. Morisaki, H. Suzuki, C. Takahashi, S. Sakakibara, K. Watanabe, T. Watanabe, T. Minami, S. Morita, K. Tanaka, S. Ohdachi, S. Kubo, N. Inoue, H. Yamada, K. Nishimura, S. Okamura, K. Matsuoka, O. Motojima, M. Fujiwara, A. Iiyoshi, C. C. Klepper, J.F. Lyon, A.C. England, D.E. Greenwood, D.K. Lee, D.R. Overbey, J.A. Rome, D.E. Schechter and C.T. Wilson,
Edge Plasma Control by a Local Island Divertor in the Compact Helical System; Sep. 1996 (IAEA-CN-64/C1-2)

NIFS-439 K. Ida, K. Kondo, K. Nagaski T. Hamada, H. Zushi, S. Hidekuma, F. Sano, T. Mizuuchi, H. Okada, S. Besshou, H. Funaba, Y. Kurimoto, K. Watanabe and T. Obiki,
Dynamics of Ion Temperature in Heliotron-E; Sep. 1996 (IAEA-CN-64/CP-

5)

NIFS-440 S. Morita, H. Idei, H. Iguchi, S. Kubo, K. Matsuoka, T. Minami, S. Okamura, T. Ozaki, K. Tanaka, K. Toi, R. Akiyama, A. Ejiri, A. Fujisawa, M. Fujiwara, M. Goto, K. Ida, N Inoue, A. Komori, R. Kumazawa, S. Masuzaki, T. Morisaki, S. Muto, K. Narihara, K. Nishimura, I. Nomura, S. Ohdachi, M.. Osakabe, A. Sagara, Y. Shirai, H. Suzuki, C. Takahashi, K. Tsumori, T. Watari, H. Yamada and I. Yamada,
A Study on Density Profile and Density Limit of NBI Plasmas in CHS; Sep. 1996 (IAEA-CN-64/CP-3)

NIFS-441 O. Kaneko, Y. Takeiri, K. Tsumori, Y. Oka, M. Osakabe, R. Akiyama, T. Kawamoto, E. Asano and T. Kuroda,
Development of Negative-Ion-Based Neutral Beam Injector for the Large Helical Device; Sep. 1996 (IAEA-CN-64/GP-9)

NIFS-442 K. Toi, K.N. Sato, Y. Hamada, S. Ohdachi, H. Sakakita, A. Nishizawa, A. Ejiri, K. Narihara, H. Kuramoto, Y. Kawasumi, S. Kubo, T. Seki, K. Kitachi, J. Xu, K. Ida, K. Kawahata, I. Nomura, K. Adachi, R. Akiyama, A. Fujisawa, J. Fujita, N. Hiraki, S. Hidekuma, S. Hirokura, H. Idei, T. Ido, H. Iguchi, K. Iwasaki, M. Isobe, O. Kaneko, Y. Kano, M. Kojima, J. Koog, R. Kumazawa, T. Kuroda, J. Li, R. Liang, T. Minami, S. Morita, K. Ohkubo, Y. Oka, S. Okajima, M. Osakabe, Y. Sakawa, M. Sasao, K. Sato, T. Shimpo, T. Shoji, H. Sugai, T. Watari, I. Yamada and K. Yamauti,
Studies of Perturbative Plasma Transport, Ice Pellet Ablation and Sawtooth Phenomena in the JIPP T-IIU Tokamak; Sep. 1996 (IAEA-CN-64/A6-5)

NIFS-443 Y. Todo, T. Sato and The Complexity Simulation Group,
Vlasov-MHD and Particle-MHD Simulations of the Toroidal Alfvén Eigenmode; Sep. 1996 (IAEA-CN-64/D2-3)

NIFS-444 A. Fujisawa, S. Kubo, H. Iguchi, H. Idei, T. Minami, H. Sanuki, K. Itoh, S. Okamura, K. Matsuoka, K. Tanaka, S. Lee, M. Kojima, T.P. Crowley, Y. Hamada, M. Iwase, H. Nagasaki, H. Suzuki, N. Inoue, R. Akiyama, M. Osakabe, S. Morita, C. Takahashi, S. Muto, A. Ejiri, K. Ida, S. Nishimura, K. Narihara, I. Yamada, K. Toi, S. Ohdachi, T. Ozaki, A. Komori, K. Nishimura, S. Hidekuma, K. Ohkubo, D.A. Rasmussen, J.B. Wilgen, M. Murakami, T. Watari and M. Fujiwara,
An Experimental Study of Plasma Confinement and Heating Efficiency through the Potential Profile Measurements with a Heavy Ion Beam Probe in the Compact Helical System; Sep. 1996 (IAEA-CN-64/C1-5)

NIFS-445 O. Motojima, N. Yanagi, S. Imagawa, K. Takahata, S. Yamada, A. Iwamoto, H. Chikaraishi, S. Kitagawa, R. Maekawa, S. Masuzaki, T. Mito, T. Morisaki, A. Nishimura, S. Sakakibara, S. Satoh, T. Satow, H. Tamura, S. Tanahashi, K. Watanabe, S. Yamaguchi, J. Yamamoto, M.Fujiwara and A. Iiyoshi,
Superconducting Magnet Design and Construction of LHD; Sep. 1996 (IAEA-CN-64/G2-4)

NIFS-446 S. Murakami, N. Nakajima, S. Okamura, M. Okamoto and U. Gasparino,

Orbit Effects of Energetic Particles on the Reachable β–Value and the Radial Electric Field in NBI and ECR Heated Heliotron Plasmas; Sep. 1996 (IAEA-CN-64/CP -6) Sep. 1996

NIFS-447 K. Yamazaki, A. Sagara, O. Motojima, M. Fujiwara, T. Amano, H. Chikaraishi, S. Imagawa, T. Muroga, N. Noda, N. Ohyabu, T. Satow, J.F. Wang, K.Y. Watanabe, J. Yamamoto , H. Yamanishi, A. Kohyama, H. Matsui, O. Mitarai, T. Noda, A.A. Shishkin, S. Tanaka and T. Terai
Design Assessment of Heliotron Reactor; Sep. 1996 (IAEA-CN-64/G1-5)

NIFS-448 M. Ozaki, T. Sato and the Complexity Simulation Group,
Interactions of Convecting Magnetic Loops and Arcades; Sep. 1996

NIFS-449 T. Aoki,
Interpolated Differential Operator (IDO) Scheme for Solving Partial Differential Equations; Sep. 1996

NIFS-450 D. Biskamp and T. Sato,
Partial Reconnection in the Sawtooth Collapse; Sep. 1996

NIFS-451 J. Li, X. Gong, L. Luo, F.X. Yin, N. Noda, B. Wan, W. Xu, X. Gao, F. Yin, J.G. Jiang, Z. Wu., J.Y. Zhao, M. Wu, S. Liu and Y. Han,
Effects of High Z Probe on Plasma Behavior in HT-6M Tokamak; Sep. 1996

NIFS-452 N. Nakajima, K. Ichiguchi, M. Okamoto and R.L. Dewar,
Ballooning Modes in Heliotrons/Torsatrons; Sep. 1996 (IAEA-CN-64/D3-6)

NIFS-453 A. Iiyoshi,
Overview of Helical Systems; Sep. 1996 (IAEA-CN-64/O1-7)

NIFS-454 S. Saito, Y. Nomura, K. Hirose and Y.H. Ichikawa,
Separatrix Reconnection and Periodic Orbit Annihilation in the Harper Map; Oct. 1996

NIFS-455 K. Ichiguchi, N. Nakajima and M. Okamoto,
Topics on MHD Equilibrium and Stability in Heliotron / Torsatron; Oct. 1996

NIFS-456 G. Kawahara, S. Kida, M. Tanaka and S. Yanase,
Wrap, Tilt and Stretch of Vorticity Lines around a Strong Straight Vortex Tube in a Simple Shear Flow; Oct. 1996

NIFS-457 K. Itoh, S.-I. Itoh, A. Fukuyama and M. Yagi,
Turbulent Transport and Structural Transition in Confined Plasmas; Oct. 1996